Check for updates

Received: 2 March 2023 | Accepted: 19 June 2023
DOI: 10.1111/nrm.12381

Natural Resource Modeling WILEY

Pacific Northwest conifer forest stand carrying capacity under future climate scenarios

Ryan R. Heiderman | Mark J. Kimsey Jr.

Department of Forestry, Rangeland and Fire Sciences—Intermountain Forestry Cooperative, University of Idaho, Moscow, Idaho, USA

Correspondence
Ryan R. Heiderman, Department of Forestry, Rangeland and Fire Sciences—Intermountain Forestry Cooperative, University of Idaho, 875 Perimeter Dr. MS1133, Moscow, ID 83844-1133, USA.
Email: ryanheiderman@uidaho.edu

Abstract

Maximum stand density index (SDI_{MAX}) represents the carrying capacity of a forest stand based on the relationship between the number of trees and their size. Plot-level inventory data provided through a collaborative network of federal, state, and private forest management groups were utilized to develop SDI_{MAX} models for important Pacific Northwest conifers of western Washington and Oregon, USA. The influence of site-specific climatic and environmental variables was explored within an ensemble learning model. Future climate projections based on global circulation models under different representative CO_2 concentration pathways (RCP 4.5 and RCP 8.5) and timeframes (2050s and 2080s) were utilized in a space-fortime substitution to understand potential shifts in modeled SDI_{MAX}. A majority of the region showed decreases in carrying capacity under future climate conditions. Modeled mean SDI_{MAX} decreased 5.4% and 11.4% for Douglasfir (Pseudotsuga menziesii (Mirb.) Franco) dominated forests and decreased 6.6% and 8.9% for western hemlock (Tsuga heterophylla (Raf.) Sarg.) and Pacific silver fir (Abies amabilis), dominated forests under the RCP 4.5 in the 2050s and RCP 8.5 in the 2080s, respectively. Projected future conditions often fall outside the range of any

This is an open access article under the terms of the Creative Commons Attribution License, which permits use, distribution and reproduction in any medium, provided the original work is properly cited.
© 2023 The Authors. Natural Resource Modeling published by Wiley Periodicals LLC.

Natural Resource Modeling. 2023;36:e12381. wileyonlinelibrary.com/journal/nrm 1 of 21

https://doi.org/10.1111/nrm.12381

contemporary climate profile, resulting in what may be referred to as extramural conditions. Within the study region, 45% and 46% of climate variables included in the final model were extramural for the Douglas-fir and hemlock models, respectively, under RCP 8.5 in the 2080s. Although extrapolating beyond the range of input data is not appropriate and many unknowns remain regarding future climate projections, these results allow for general interpretations of the direction and magnitude of potential shifts in forest carrying capacity.

Recommendations for Resource Managers

- These results present forest managers and policymakers with the ability to make location-specific interpretations of potential shifts in forest stand carrying capacity under potential future climate projection scenarios, which show forest communities of the Pacific Northwest may be facing a longer, warmer, droughtier growing season.
- Across the study region, a majority of the landscape is seeing a downward shift in the modeled maximum carrying capacity under future climate projections.
- The modeled carrying capacity of mixed species stands appear to be more resilient to projected changes in climate.
- Planting and thinning to lower densities may provide resilience and capture the projected increases in densityrelated mortality.
- Across all projected future climate scenarios fall into extramural conditions, which are a combination of climatic conditions not currently experienced in the study area.

KEYWORDS

carrying capacity, climate change, Douglas-fir, gradient boosting regression, maximum stand density index, Pacific Northwest, western hemlock

19397445, 2023, 4, Downloaded from https://onlinelibrary.wiley.com/doi/10.1111/nrm.12381, Wiley Online Library on [29/11/2023]. See the Terms and Conditions (https://onlinelibrary.wiley.com/terms-and-conditions) on Wiley Online Library for rules of use; OA articles are governed by the applicable Creative Commons License

19397445, 2023, 4, Downloaded from https://onlinelibrary.wiley.com/doi/10.1111/nrm.12381, Wiley Online Library on [29/11/2023]. See the Terms and Conditions (https://onlinelibrary.wiley.com/terms-and-conditions) on Wiley Online Library for rules of use; OA articles are governed by the applicable Creative Commons License

1 | INTRODUCTION

Forest stands are generally adapted to the environmental conditions that they have been exposed to throughout stand development. Changes to temperature, humidity, and timing and amount of precipitation are all predicted to occur in the near and distant future (IPCC, 2013). General Circulation Models (GCMs) with different greenhouse gas emissions scenarios (representative CO_2 concentration pathways [RCPs]) project various changes to these important climate variables (Wang et al., 2016). These potential changes will impact biogeochemical cycles between forests and the environment, which may lead to changes in forest growth, survival, and structure (Chmura et al., 2011). The development of adaptive forest management strategies for potential future climatic conditions may provide resilience to a changing environment.

Forests of the Pacific Northwest, in particular, rely on water storage in snowpack and soils during summer droughts common to the Mediterranean climate experienced in the region (Franklin & Waring, 1980). Even without changes to the total amount of precipitation, earlier snowmelt and a decline in precipitation falling as snow (PAS) are reducing this critically important water reservoir, and further intensifying water stress (Harpold, 2016). The manipulation and control of growing stock, in the form of density management, could be a key silvicultural tool to increase forest resilience to environmental change. Reducing stand density increases water and other resources available to the residual trees, and in turn, results in increased tree vigor and a greater ability to handle drought, and damage from insects and disease (Puettmann, 2011). Tree species and forest types that may be more vulnerable to changes in temperature or precipitation patterns, in particular overstocked stands or those with high levels of competition, should be targeted for density management manipulations (Chmura et al., 2011).

An understanding of the current and potential future responses of forests is necessary to facilitate the development of silvicultural management options for adaptation to any degree of future change (Dolanc et al., 2013). The response a forest may have to a changing climate will ultimately depend on local, site-specific conditions. Special concern should be given toward areas where species grow at a moisture-limited range of conditions (Puettmann, 2011). Decision-makers should target the most vulnerable sites, life stages, traits, and processes to increase forest adaptability (Chmura et al., 2011). For example, the negative impacts of declining snowpack can be exacerbated by high stand density. Gleason et al. (2021) recommend reducing stand density as a mitigation strategy to promote resilience to snow droughts in ponderosa pine stands and Fernandes et al. (2016) found thinning in pine stands increased the resilience to climate variations by increasing water use efficiency and promoted targeted (i.e., under appropriate timing) density reduction as an effective adaptive silviculture strategy under a changing climate.

Knowledge of where vulnerable species and forest types are found, such as areas with drought concerns, will facilitate where climate adaptation management efforts should be directed. Some management adjustments might include modifying harvest schedules and thinning regimes, or choosing different species or genetics when replanting (Millar et al., 2007). Capturing mortality before the initiation of self-thinning (i.e., density-dependent mortality) requires temporal knowledge of when limiting conditions will begin to impact stand development.

It has been demonstrated through empirical statistical analysis that climatic conditions affect the carrying capacity (maximum stand density index [SDI_{MAX}]) of a forest stand, which may be predicted through modeling efforts (Aguirre et al., 2018; Andrews et al., 2018; Kimsey et al., 2019). Due to the climatic sensitivity of SDI_{MAX}, this index may be used to assess climate change adaptation and

mitigation efforts (Brunet-Navarro et al., 2016). One approach to understanding how future conditions may affect modeled SDI_{MAX} is to utilize projected climatic conditions in place of historical climate data used to build the original models, referred to as space-for-time substitution (Yue et al., 2016). While these statistical models are correlative, and not necessarily suited to make mechanistic interpretations, they do allow the relative importance of climatic predictor variables to be assessed (Rehfeldt et al., 2006).

Statistical analysis techniques such as ensemble learning methods (i.e., random forest and stochastic gradient boosting) allow for the effect of many variables and their interactions on the target function to be assessed (Friedman, 2001; Iverson et al., 2008). Nonparametric, ensemble learning methods are ideal for large data sets with a multidimensional variable space with no prior distribution assumed between dependent and independent variables (Andrews et al., 2018). The ability of a model to incorporate many variables has proved useful in projecting the effects of climate change on trees and forests (Chmura et al., 2011).

Future scenarios are often outside the range of any contemporary climate profile. These projections may be considered extramural (Rehfeldt et al., 2006) or no-analog conditions (Puettmann, 2011). Thus, any predictions made by models relying on future projections are not defensible. Rehfeldt et al. (2006) found among most of the biotic communities they examined that the majority of the landscape was projected into an extramural condition by the year 2100, with some reaching over 85%. Climate conditions were considered extramural if any one of the predictor variables at a location was outside the range of contemporary conditions. With this in mind, interpretations regarding the direction and magnitude of change may still be valid to consider. Exploring a variety of timescales and emissions scenarios can give a summary of the expected range and variability of any future changes.

The goal of this study is to understand the relationship between SDI_{MAX} and future climatic conditions across the Pacific Northwest forest region. Specific objectives are to: (1) utilize linear quantile mixed models (LQMMs) to determine the self-thinning boundary of important forest types and tree species, (2) determine climatic variable influence and importance utilizing gradient boosting methodology (GBM) to predict SDI_{MAX}, (3) estimate potential future directional shifts in SDI_{MAX} under various climate projections using GCMs and different RCPs, and (4) understand what proportion of the future projections for the study area falls into extramural or no-analog conditions.

2 | MATERIALS AND METHODS

2.1 | Plot data: Inventory data sets

Forest inventory plot data for this project were provided by a collaborative network of public and private land management agencies, the Intermountain Forestry Cooperative, and the United State's Forest Service Forest Inventory and Analysis program. Each plot record contained the important tree metrics of quadratic mean diameter (QMD), number of trees per hectare (TPH) and proportion of basal area by major species group. Each record contained precise plot coordinates, which allowed for the extraction of important site-specific, environmental variables from geospatial layers. Data screening removed plots with less than 2.54 cm QMD and 24.7 TPH to establish a consistent threshold of diameter and number of trees. Only trees marked as living were included in plot-level estimates. The final data set consisted of 168,220 unique and statistically independent (i.e., no remeasured plots or stands) observations representing the varied range of forest ecotypes across the Pacific Northwest.

19397445, 2023, 4, Downloaded from https://onlinelibrary.wiley.com/doi/10.1111/nrm.12381, Wiley Online Library on [29/11/2023]. See the Terms and Conditions (https://onlinelibrary.wiley.com/terms-and-conditions) on Wiley Online Library for rules of use; OA articles are governed by the applicable Creative Commons License

19397445, 2023, 4, Downloaded from https://onlinelibrary.wiley.com/doi/10.1111/nrm.12381, Wiley Online Library on [29/11/2023]. See the Terms and Conditions (https://onlinelibrary.wiley.com/terms-and-conditions) on Wiley Online Library for rules of use; OA articles are governed by the applicable Creative Commons License

Plot records were subset to fall into one of two categories, the first (n = 155,083) are those plots containing at least 10% Douglas-fir (Pseudotsuga menziesii (Mirb.) Franco) by basal area, and the second (n = 13,137) consisting of plots with at least 10% western hemlock (Tsuga heterophylla (Raf.) Sarg.) basal area that contained no Douglas-fir proportion. This second subset of data points was concentrated in the more niche environments in the Coast Range, Olympic Peninsula, and Northern Cascades where wetter, climax forest conditions with less extreme weather events are found. Whereas Douglas-fir tends to be more generally found across the study area and provides a good basis for the average conditions. These data sets will be referred to as DF-Mix and HemFir, respectively.

2.2 | Topographic data

Topographic attributes were derived from the US Department of Agriculture (USDA) and National Resource Conservation Service (NRCS) National Elevation Data 30-m digital elevation models. Slope and aspect were derived using the "raster" package (Hijmans, 2020) available through R 4.0 (R Core Team, 2020). Trigonometric transformations and interactions of cosine, sine, and tangent on slope and aspect were utilized to express the influence of these features on climate factors such as moisture and temperature (Roise & Betters, 1981). Spatial maps of soil parent materials were derived from USGS 1:24,000 geology maps and surficial volcanic ash mantles from the NRCS soil survey geographic database (SSURGO). Major geologic groupings and presence/absence of ash influence are broad categorical descriptors that serve as proxies of regional nutritional and water-holding capacity features, which are important drivers affecting growth and mortality (Kimsey et al., 2019). These categorical groupings included eight major soil parent materials including extrusive, intrusive, glacial, metamorphic, metasedimentary, sedimentary, surficial deposits, and sandstone; and a presence/absence of categorical variable for surficial ash influence.

2.3 | Climatic data

Climate data were obtained through the ClimateNA v6.11 software package using plot-specific latitude, longitude, and elevation. ClimateNA downscales historical and future climate data layers into scale-free (not gridded but directly estimable for any location) point estimates of climate values for the entire North American continent (Wang et al., 2016). These climate data contain directly calculated and derived variables, as well as various interactions resulting in over 230 climate variables available for extraction. Given the typical timeframe needed for a tree to grow to the data set mean of 29 cm diameter at breast height, 30-year (1961–1990) climate normals were utilized to represent the average conditions these forests experienced during stand development. Future projections within ClimateNA are based on GCMs of the Climate Model Intercomparison Project 5. This analysis utilizes the 15 CGM ensemble, composed of the following Atmosphere-Ocean GCMs: ACCESS1-0 (Australia), CCSM4 (National Center for Atmospheric Research, USA), CESM1-CAM5 (University Center for Atmospheric Research, USA), CNRM-CM5 (France), CSIRO-Mk3-6-0 (Australia), CanESM2 (Canada), GFDL-CM3 (Geophysical Fluid Dynamics Lab, USA), GISS-E2R (Goddard Institute of Space Studies, USA), HadGEM2-ES (United Kingdom), INM-CM4 (Russia), IPSL-CM5A-MR (France), MIROC-ESM (Japan), MIROC5 (Japan), MPI-ESM-LR (Germany), and MRI-CGCM3 (Japan). The future projections incorporate different greenhouse gas concentration trajectories or

RCPs. This analysis selected two RCPS: RCP 4.5, a medium stabilization scenario where emissions peak in the 2040s with radiative forcing pathways stabilizing at 6 W/m^2 (~650 ppm CO_2) after 2100, and RCP 8.5, a very high emission scenario with rising radiative forcing pathway leading to 8.5 W/m^2 (~1370 ppm CO_2) by the end of the century (Vuuren et al., 2011). Each 15 GCM ensemble and RCP scenario were summarized into 30-year time future periods, referred to hereafter as 2050s (2041–2070) and 2080s (2071–2100).

From each of the DF-Mix and HemFir data sets, four different future climate scenarios were built. While keeping the tree and topographic data constant, future climate variables were extracted for each plot location for the four climate scenarios RCP 4.5 in period 2050s, RCP 4.5 in period 2080s, RCP 8.5 in period 2050s, and RCP 8.5 in period 2080s. These additional climate extractions resulted in five scenarios for each DF-Mix and HemFir data sets: the historical data set and four future scenarios. Comparisons of predicted SDI_{MAX} between the future and the historical climate scenarios were evaluated.

2.4 | Statistical analysis: LQMM and GBM

To understand the influence of climate on forest stand carrying capacity, first the maximum size–density relationship (SDI_{MAX}) must be estimated. Following the findings of Salas-Eljatib and Weiskittel (2018), LQMMs were developed with the "lqmm" package (Geraci, 2014) within the R programming environment (R Core Team, 2020) to estimate the random plot-specific intercepts and fixed species-specific slope of the self-thinning line based on the Reineke (1933) equation:

$$\ln TPH = (\beta_0 + k_i) + \beta_1 \ln QMD,$$

where β_0 and β_1 are fixed effects parameters and k_i is the estimated random effect for plot record i. The random intercept parameter produced unique individual plot-level intercept values, thus giving each record a unique SDI_{MAX}, where SDI_{MAX} is the maximum number of TPH when QMD is equal to 10 cm. As in Andrews et al. (2018), values from the 90th through the 99th quantile were compared to determine which percentile to utilize. The 95th was chosen as the values produced were reasonable while removing the sensitivity of highly influential observations found at the higher quantiles, as well as unreasonably low values produced at the lower quantiles.

The next step introduces site-specific variables by linking the estimated SDI_{MAX} to climatic and other environmental properties found at each plot location. Utilizing the ensemble learning technique GBM, variable influence and importance were assessed. Stochastic gradient boosting (GBM) makes use of an additive gradient descent "boosting" algorithm that builds successively improved prediction trees (Friedman, 2001). Each data set, DF-Mix and HemFir, was split 70/30 into training and testing sets. The test set was held back from model development and used as independent validation of model fit. The R packages "gbm" (Greenwell et al., 2020) and "caret" (Kuhn, 2020) were used to determine the influence of environmental variables by tuning a GBM model. The GBM model was tuned using a grid search method, where the various parameters were optimized toward the best predictive model. GBM constructs an ensemble of prediction trees in a "greedy stepwise" manner and is noted for being robust to the collinearity of variables (Hastie et al., 2008). A first run included all variables. Then, variable importance, the relative influence of variables on prediction, was examined to reduce the

19397445, 2023, 4, Downloaded from https://onlinelibrary.wiley.com/doi/10.1111/nrm.12381, Wiley Online Library on [29/11/2023]. See the Terms and Conditions (https://onlinelibrary.wiley.com/terms-and-conditions) on Wiley Online Library for rules of use; OA articles are governed by the applicable Creative Commons License

number of variables in the model to only the most influential. A relative influence of 0.25 was chosen to remove noninformative variables from the first-run predictor set. Simplifying the predictor set results in a more parsimonious model, without degradation of model fit (Elith et al., 2008). Final models were selected based on a 5-fold, cross-validated mean absolute error (MAE). MAE for both training and testing data was assessed to prevent overfitting. The final number of model-built trees producing the lowest error on testing data without overfitting was chosen.

2.5 | Additional regionwide data sets

In addition to the inventory plot-driven data sets, a 1-km hexagonal grid was placed across the entire study region and then clipped to each Douglas-fir and western hemlock range. Species ranges were determined from FIA interpolated basal area maps, where if at least 10% of the total basal area found at any given location was of the species of interest, then that location was considered in range. The grid across the entire regionwide area was then clipped to the ranges creating two regionwide data sets for DF-Mix (n = 151,299) and HemFir (n = 80,974).

The same topographic and climate variables were extracted for each plot location, including the four future scenarios. The final GBM model for DF-Mix and HemFir was then applied to the regional grid data sets for SDI_{MAX} predictions to allow climate change scenarios to be evaluated across the entire study region. Two basal area proportion scenarios were explored, one based on pure (100% basal area proportion) Douglas-fir or western hemlock composition and a second based on species averages calculated from the original inventory plot data sets (Table 1).

TABLE 1 Species basal area proportions from the inventory data sets.

Variable	Mean	SD	Minimum	Maximum
DF-Mix				
Douglas-fir	0.77	0.27	0.10	1
Western hemlock	0.09	0.18	0	0.90
Red alder	0.05	0.15	0	0.90
Western red cedar	0.02	0.07	0	0.90
Other conifer	0.04	0.12	0	0.90
Other hardwood	0.03	0.11	0	0.90
HemFir				
Douglas-fir	0	0	0	0
Western hemlock	0.68	0.30	0.10	1
Red alder	0.13	0.23	0	0.90
Western red cedar	0.04	0.12	0	0.90
Other conifer	0.13	0.23	0	0.90
Other hardwood	0.02	0.09	0	0.90

19397445, 2023, 4, Downloaded from https://onlinelibrary.wiley.com/doi/10.1111/nrm.12381, Wiley Online Library on [29/11/2023]. See the Terms and Conditions (https://onlinelibrary.wiley.com/terms-and-conditions) on Wiley Online Library for rules of use; OA articles are governed by the applicable Creative Commons License

2.6 | Extramural conditions

Future climate projections under the various scenarios were compared to the historical conditions to understand how much of the landscape falls into extramural conditions under future projections. Utilizing the regionwide data sets, all climate variables included in the DFMix and HemFir final models were evaluated for extramural status by comparing each of the future scenario predictions to the historical conditions at the same location. A variable value that falls outside (i.e., greater than or equal to the minimum or maximum values) the range of the historical climate data is marked as extramural. Two instances were evaluated, first, whether any of the variables at a given point fell outside the range, and second, what proportion of the variables at any given point fell outside the range. Each was evaluated as falling within the absolute range as well as within 5% and 10% of the absolute range.

3 | RESULTS

3.1 | Maximum size–density relationship

The LQMM analysis fits a self-thinning outer boundary line to the 95th quantile of data points. This resulted in a self-thinning slope of −1.608 and −1.544 for the DF-Mix and HemFir data sets, respectively. The random intercept produced a mean predicted SDI_{MAX} of 1220 TPH (SD = 119) with a 1%–99% quantile range from 840 to 1450 TPH for DF-mix and mean predicted SDI_{MAX} of 1396 TPH (SD = 151) with a range of 941–1681 TPH for HemFir.

3.2 | GBM model performance and variable influence on SDI_{MAX}

The final GBM model for the DF-mix data set had 4202 model learning trees and included 86 variables with a training and testing MAE of 72.5 and 77.5 TPH, respectively. The most influential variable was the Douglas-fir basal area proportion (i.e., how much of the total basal area was made up of Douglas-fir vs. other species), followed by other species basal area proportion, in particular western hemlock. Topographic variables, elevation, and the latitude and longitude at plot locations were important and highly ranked. Influential climate variables included interactions between the various measures of precipitation and temperature.

The final GBM model for the HemFir data set had 1915 model learning trees and included 106 predictor variables with a training and testing MAE of 77.0 and 104.2 TPH, respectively. The top variable was the basal area proportion of western hemlock, followed by the slope and aspect transformations, elevation, and latitude and longitude of the plot location. The most influential climate variables were similar to those included in the DF-Mix model and included various measures of precipitation timing and amount, as well as interactions of precipitation with temperature. The number of degree days above 5°C (DD5) and below 18°C (DD_18) both annually and seasonally were common variables included in the model. The summer season Hargreaves climatic moisture deficit ranked as a highly influential variable as well. The most influential variables of the chosen final GBM models for SDI_{MAX} predictions are shown in Figure 1a and Figure 1b for DF-Mix and HemFir, respectively.

19397445, 2023, 4, Downloaded from https://onlinelibrary.wiley.com/doi/10.1111/nrm.12381, Wiley Online Library on [29/11/2023]. See the Terms and Conditions (https://onlinelibrary.wiley.com/terms-and-conditions) on Wiley Online Library for rules of use; OA articles are governed by the applicable Creative Commons License

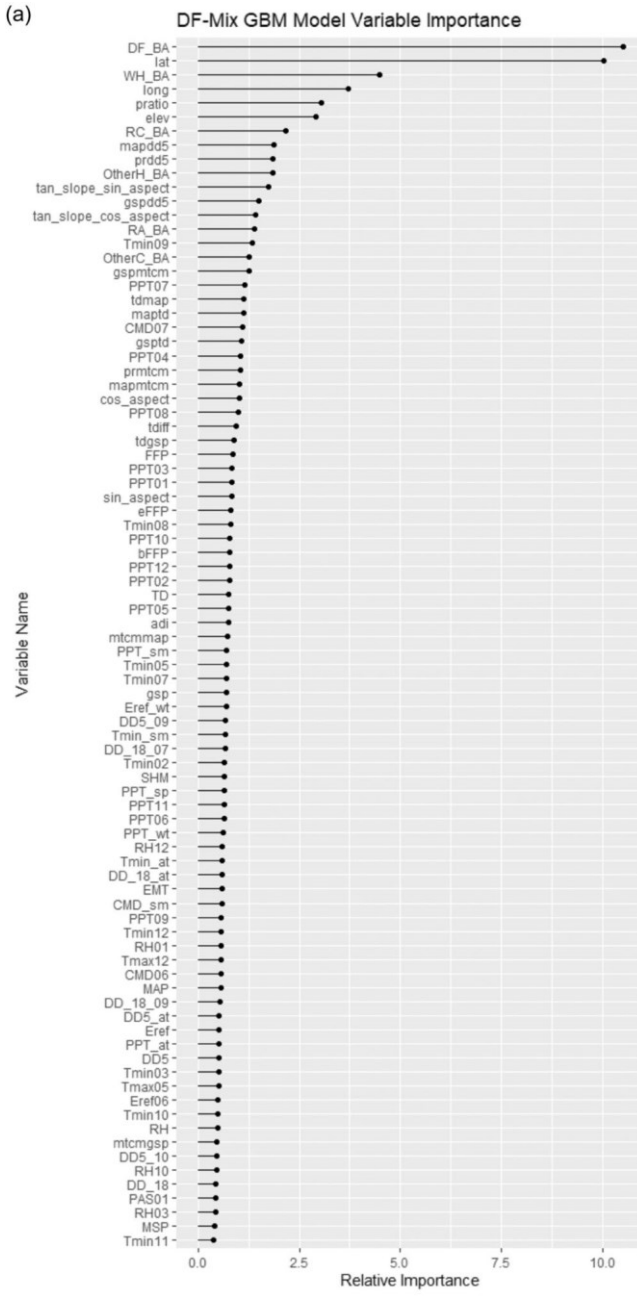

FIGURE 1 (a) Relative variable importance for the gradient boosting model for the DF-Mix data set. Important variable acronyms are defined in the appendices. (b) Relative variable importance for the gradient boosting model for the HemFir data set. Important variable acronyms are defined in the appendices.

3.3 | Future GBM model predictions: Inventory data sets

The future scenario inventory data sets were run through the final GBM model to produce predicted SDI_{MAX} under future climate conditions in the 2050s and 2080s. Both the DF-Mix and

19397445, 2023, 4, Downloaded from https://onlinelibrary.wiley.com/doi/10.1111/nrm.12381, Wiley Online Library on [29/11/2023]. See the Terms and Conditions (https://onlinelibrary.wiley.com/terms-and-conditions) on Wiley Online Library for rules of use; OA articles are governed by the applicable Creative Commons License

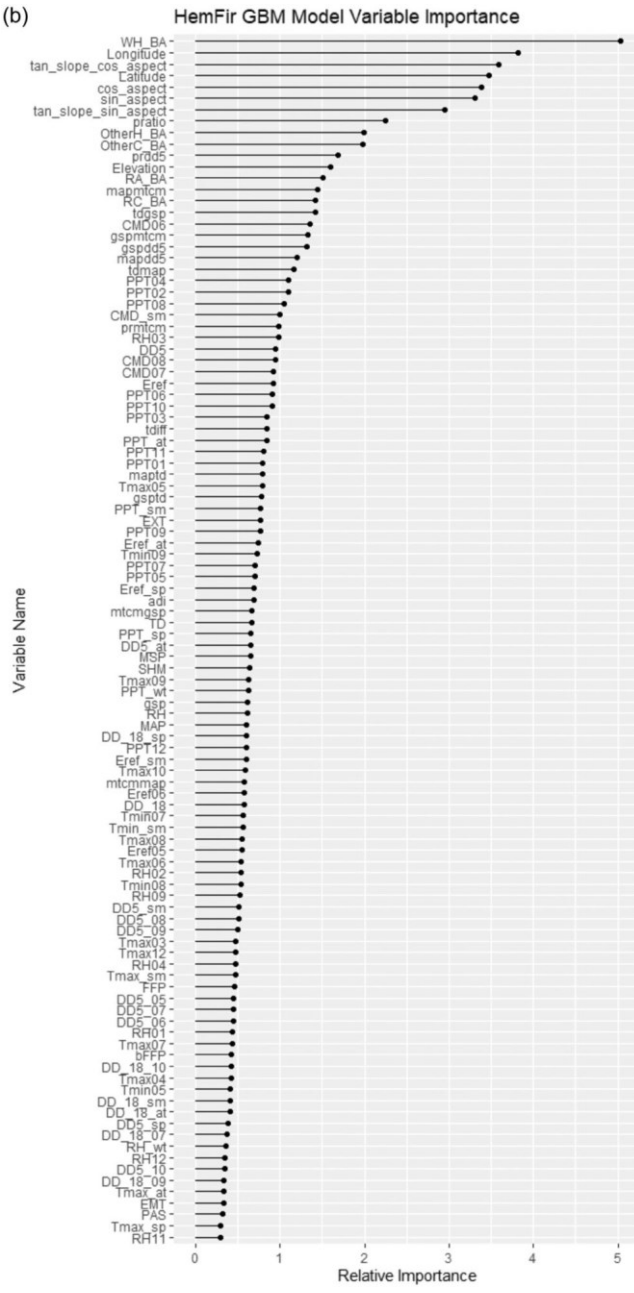

FIGURE 1 (Continued)

the HemFir data sets saw the average SDI_{MAX} value shift downward under all scenarios (Table 2).

Although the majority of SDI_{MAX} projections decreased under future conditions (at least 78%+ of records under all scenarios showed negative change), there was a range of positive and negative changes (Table 3). A small proportion of sites are projected to have favorable climatic changes, which may lead to increases in carrying capacity. Overall, the DF-Mix locations are

19397445, 2023, 4, Downloaded from https://onlinelibrary.wiley.com/doi/10.1111/nrm.12381, Wiley Online Library on [29/11/2023]. See the Terms and Conditions (https://onlinelibrary.wiley.com/terms-and-conditions) on Wiley Online Library for rules of use; OA articles are governed by the applicable Creative Commons License

TABLE 2 Average ratios of the GBM predicted SDI_{MAX} under each future scenario relative to the current SDI_{MAX} predicted with LQMM under past climate conditions for the inventory data set.

	Ratio of GBM prediction to LQMM			
	DF-Mix		HemFir	
Prediction scenario	Mean	SD	Mean	SD
Current	1.01	0.09	1.01	0.10
RCP 4.5—2050s	0.95	0.11	0.93	0.12
RCP 4.5—2080s	0.93	0.11	0.92	0.12
RCP 8.5—2050s	0.92	0.11	0.93	0.12
RCP 8.5—2080s	0.89	0.11	0.91	0.12

Note: For example, a value of 0.92 in the future scenario mean refers to the overall average future prediction in the GBM model was 8% lower relative to the current predicted in the LQMM model. The 1.01 in the current predicted mean value with the GBM model was 1% greater relative to the LQMM predicted value.

Abbreviations: GBM, gradient boosting methodology; LQMM, linear quantile mixed model; RCP, representative CO_2 concentration pathway; SDI_{MAX}, maximum stand density index.

TABLE 3 Average percent change in SDI_{MAX} for inventory data sets.

	DF-Mix			HemFir		
Scenario	Overall (%)	If+ (%)	If− (%)	Overall (%)	If+ (%)	If− (%)
RCP 4.5—2050s	−5.4	9.4	−9.7	−6.6	10.8	−11.4
RCP 4.5—2080s	−7.2	9.5	−11.0	−7.5	10.9	−12.0
RCP 8.5—2050s	−7.8	9.6	−11.5	−7.1	10.8	−11.7
RCP 8.5—2080s	−11.4	9.8	−14.2	−8.9	10.9	−12.9

Note: Overall is the mean percent change; If+ is the average change for records that showed positive change; If− is the average change for records that showed negative change.

Abbreviations: RCP, representative CO_2 concentration pathway; SDI_{MAX}, maximum stand density index.

projected to be slightly more resilient under the RCP 4.5 scenarios compared to the HemFir sites, but under the RC P8.5 scenarios, it is the reverse, with HemFir fairing marginally better overall compared to the DF-Mix sites. Not unexpectedly, the 2080s under RCP 8.5 saw the most dramatic shifts in SDI_{MAX} relative to the current with an average 11.4% and 8.9% shift downward in the mean predicted SDI_{MAX} for DF-Mix and HemFir scenarios, respectively.

19397445, 2023, 4, Downloaded from https://onlinelibrary.wiley.com/doi/10.1111/nrm.12381, Wiley Online Library on [29/11/2023]. See the Terms and Conditions (https://onlinelibrary.wiley.com/terms-and-conditions) on Wiley Online Library for rules of use; OA articles are governed by the applicable Creative Commons License

3.4 | Future GBM model predictions: Regionwide data sets

The regionwide data sets under future scenarios followed similar patterns of results as the inventory data sets. Both the DF-Mix and HemFir data sets under the 100% pure basal area and the average species basal area scenarios saw overall majority decreases in SDI_{MAX} under all future climate projections (Table 4). The scenarios with 100% basal area of Douglas-fir and western hemlock had greater magnitude in both positive and negative shifts in SDI_{MAX} compared to the average basal area scenarios. The pure basal area scenarios had a greater

TABLE 4 Average ratios (mean, 1, and 99 percentiles) and standard deviations of predicted SDI_{MAX} under each future climate scenarios relative to the current SDI_{MAX} under past climate conditions for the regionwide data set.

	DF-Mix				HemFir			
	100% Douglas-fir basal area				100% Western hemlock basal area			
Prediction scenario	Mean	SD	1%	99%	Mean	SD	1%	99%
Current	1	0	1	1	1	0	1	1
RCP 4.5—2050s	0.93	0.07	0.79	1.09	0.94	0.07	0.80	1.09
RCP 4.5—2080s	0.91	0.07	0.77	1.10	0.93	0.07	0.80	1.08
RCP 8.5—2050s	0.90	0.07	0.77	1.10	0.93	0.07	0.80	1.08
RCP 8.5—2080s	0.86	0.07	0.72	1.07	0.91	0.07	0.78	1.08
	Average species basal area proportion							
Current	1	0	1	1	1	0	1	1
RCP 4.5—2050s	0.97	0.04	0.88	1.06	0.96	0.04	0.87	1.05
RCP 4.5—2080s	0.96	0.04	0.87	1.06	0.95	0.04	0.86	1.04
RCP 8.5—2050s	0.95	0.04	0.87	1.06	0.95	0.04	0.87	1.04
RCP 8.5—2080s	0.93	0.05	0.83	1.05	0.94	0.04	0.85	1.04

Abbreviations: RCP, representative CO_2 concentration pathway; SDI_{MAX}, maximum stand density index.

proportion of sites seeing a downward shift of SDI_{MAX} compared to the average species basal area scenarios under all future climate projections.

3.5 | Extramural conditions

Extramural, or no-analog conditions, were found within all future scenarios. The percent of locations that had at least one variable falling outside the absolute range found in the historical climate conditions ranged from 49% of locations in the 2050s under RCP 4.5 scenario to 97% in the 2080s under RCP 8.5 scenario for the DF-Mix regionwide data set, and 38% to 99% for the HemFir mix under the same scenarios, respectively (data not shown). For the same time period and RCP scenarios, the average percent of all variables at each location falling outside the absolute range of historical

19397445, 2023, 4, Downloaded from https://onlinelibrary.wiley.com/doi/10.1111/nrm.12381, Wiley Online Library on [29/11/2023]. See the Terms and Conditions (https://onlinelibrary.wiley.com/terms-and-conditions) on Wiley Online Library for rules of use; OA articles are governed by the applicable Creative Commons License

climate conditions ranged from 7% to 45% for the DF-Mix and 7% to 46% for the HemFir, with these percentages dropping by roughly half when expanding the absolute range by 10% (Table 5).

Projections of future climate are impacting modeled stand carrying capacity in significant ways. Across the study region, a majority of the landscape is seeing a downward shift in the SDI_{MAX} (Figure 2a,b). This change is driven by changes in temperature (Appendix A1) and precipitation (Appendix A2). While the total amount of mean annual precipitation is projected to remain fairly constant or increase slightly under all future scenarios, the timing of precipitation is shifting away from the growing season. The balance of precipitation in the growing season relative to the entire year (PRATIO) is declining across the region, while at the same time, the frost-free period and both summer and winter temperatures are increasing.

TABLE 5 Average percent of explanatory variables for each record that falls outside the range of historical climate conditions.

	DF-Mix		HemFir	
	Average percent of explanatory variables falling outside...		Average percent of explanatory variables falling outside...	
Scenario	Abs current range	10% of current range	Abs current	10% of range current range
RCP 4.5—2050s	7%	1%	7%	1%
RCP 4.5—2080s	15%	3%	14%	4%
RCP 8.5—2050s	17%	4%	16%	5%
RCP 8.5—2080s	45%	21%	46%	25%

Note: Two categories of extramural are shown: Abs is the percent of variables outside the absolute range of current climate and 10% is the average percent of variables outside 10% of the absolute range.

Abbreviations: RCP, representative CO_2 concentration pathway.

Average temperatures in both the coldest and warmest months are projected to increase by 2–3°C under the RCP 4.5—2050s projection, and by as much as 4–6°C under the RCP 8.5— 2080s projection. Forests are being exposed to an earlier, longer, warmer growing season with access to a smaller amount of precipitation. Water storage in the form of snowpacks is extremely important for forests growing in droughty summer conditions (Gleason et al., 2021; Waring & Franklin, 1979). The amount of PAS is projected to dramatically decline (Klos et al., 2014), further exacerbating the limited amount of water these forests have access to during the low-precipitation summers. Stand carrying capacity is almost exclusively determined by competition for water resources while under severe drought (Deng et al., 2006) and with future conditions expected to become more water-limiting for Pacific Northwest forests, a drop in SDI_{MAX} is expected.

4 | DISCUSSION

Higher elevation sites and those closer to the Pacific Northwest coast are not seeing as dramatic a shift in predictions compared to the lower elevation, inland sites found in the Willamette Valley, which are

19397445, 2023, 4, Downloaded from https://onlinelibrary.wiley.com/doi/10.1111/nrm.12381, Wiley Online Library on [29/11/2023]. See the Terms and Conditions (https://onlinelibrary.wiley.com/terms-and-conditions) on Wiley Online Library for rules of use; OA articles are governed by the applicable Creative Commons License

almost exclusively in the negative direction. The magnitude of change projections in temperature, precipitation timing, and precipitation as snow is buffered by higher elevation. Competition for water resources will not be as extreme in these areas and in fact, may see an increase in stand carrying capacity due to the increase in growing season length. Way and Oren (2010) suggest that high-altitude tree communities may benefit from some degree of warming as opposed to warm-adapted species often found at the edges of moisture-limited environments. The results found in this study seem to agree with this and other projections of general range shifts upward in elevation with anticipated changes in climate (Parmesan, 2006; Reheldt et al., 2006). The impact of future climate changes on stand carrying capacity will be location dependent and any management decisions need to account for the specificity.

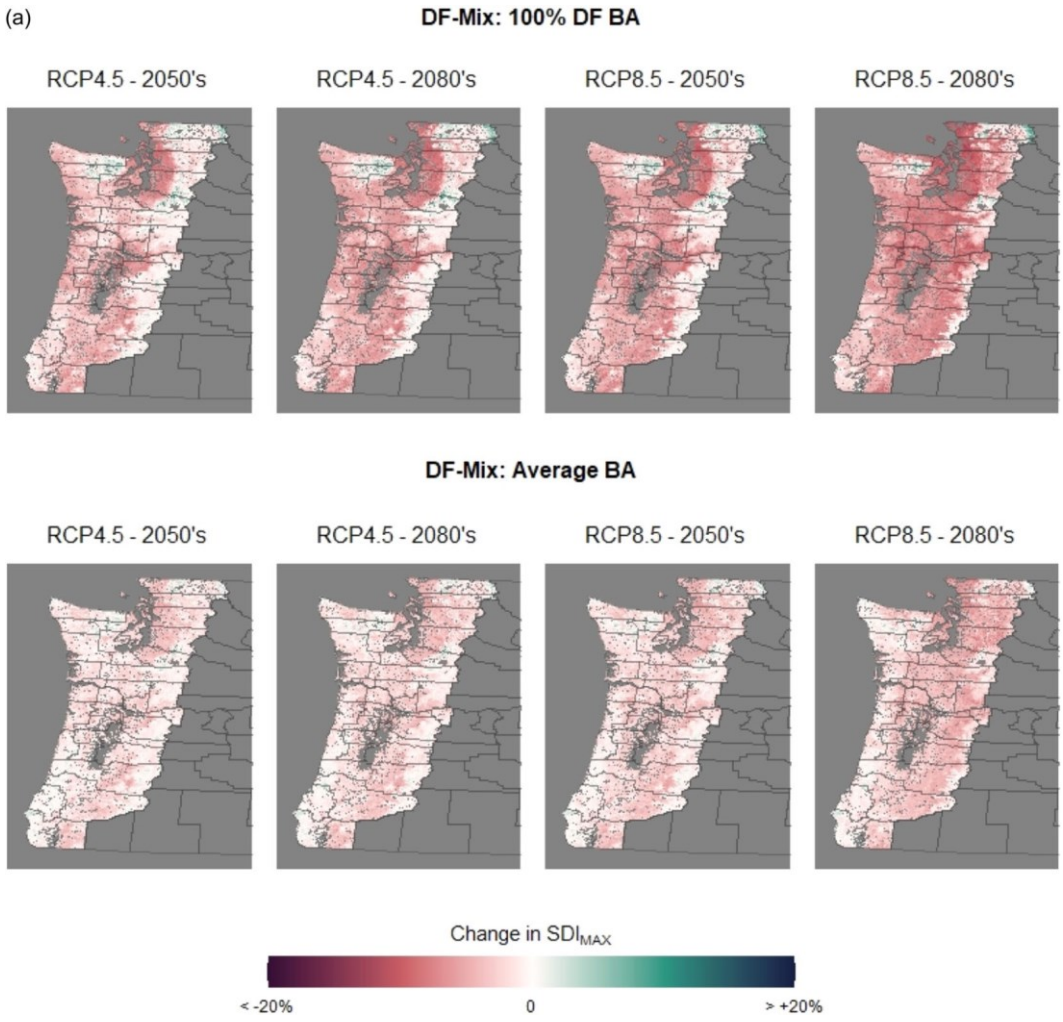

FIGURE 2 (a) Percent change in maximum stand density index (SDI_{MAX}) for regionwide DF-Mix range under future climate scenarios relative to current. Resolution of 1 km hexagonal raster tiles. (b)Percent change in SDI_{MAX} for regionwide HemFir range under future climate scenarios relative to current. Resolution of 1 km hexagonal raster tiles. BA, basal area; RCP, representative CO_2 concentration pathway.

The impact of future climate on stand carrying capacity is shown to be greater in pure stands of Douglas-fir and western hemlock relative to mixed species stands. Species mixing in general has been shown to lead to increased packing density within a canopy space due to complementary ecological traits and crown geometry (Pretzsch & Biber, 2016). The modeled carrying capacity of mixed species stands appear to be more resilient to projected changes in climate. Exploring the inventory data sets, records showing projected increases in SDI_{MAX} had more diversity of species basal area proportions. For example, under RCP 8.5—2080s scenario, the DF-MIX data set showed average Douglas-fir basal area was 78% for plots with a decrease in SDI_{MAX} and 71% for plots with an increase, and for the HemFir data set, the average western hemlock basal area was 69% for records with a decrease in SDI_{MAX} and 62% for those with an increase. This relationship held for all future climate scenarios. While this in part may be

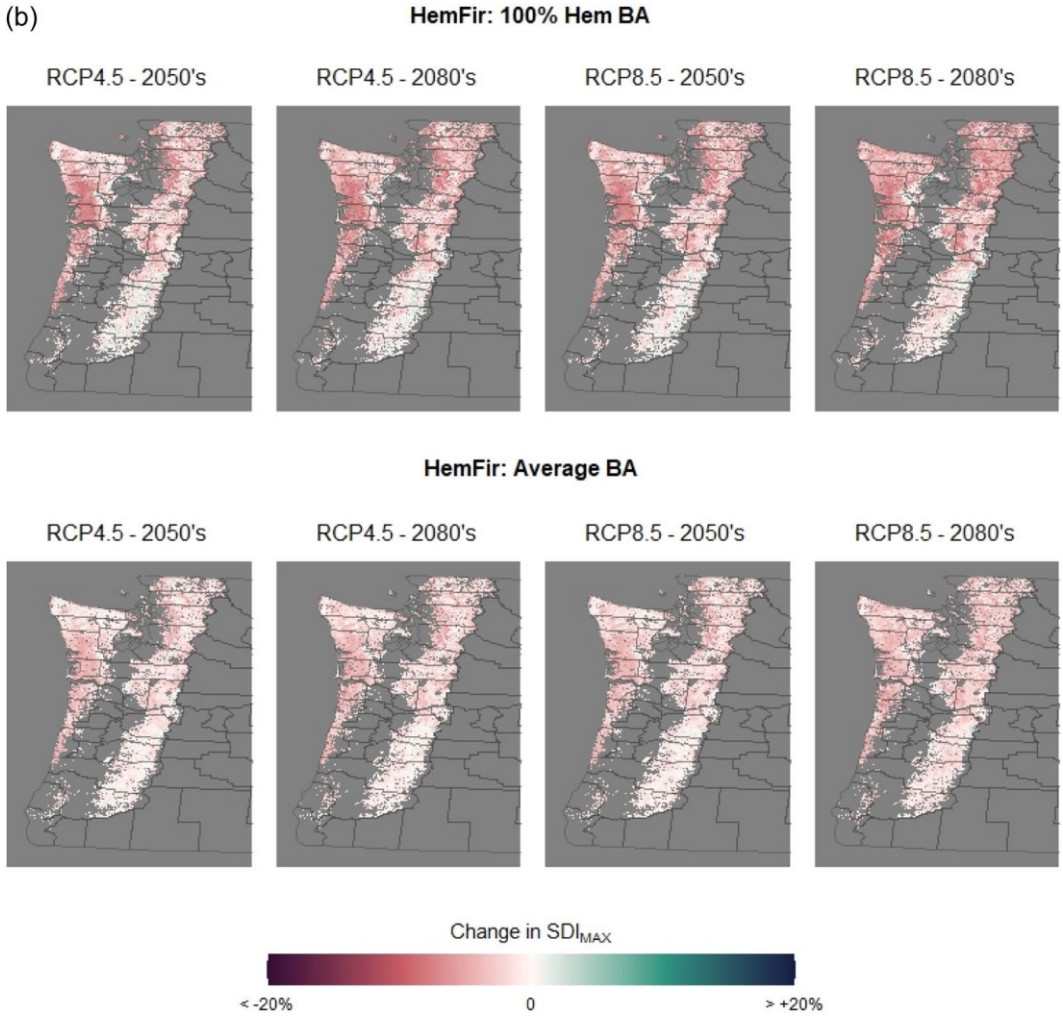

FIGURE 2 (Continued)

attributed to the GBM model, which showed more diverse plots as having overall higher SDI_{MAX}, it also shows that given changes in important climate variables, more diverse stands have a greater resiliency to the impact of these changes compared to purer stands.

19397445, 2023, 4, Downloaded from https://onlinelibrary.wiley.com/doi/10.1111/nrm.12381, Wiley Online Library on [29/11/2023]. See the Terms and Conditions (https://onlinelibrary.wiley.com/terms-and-conditions) on Wiley Online Library for rules of use; OA articles are governed by the applicable Creative Commons License

That said, exploring the regionwide data sets, the pure basal area scenarios showed the greatest magnitude shifts in SDI_{MAX} relative to the mixed species in both the positive and negative direction. Locations under pure basal area scenarios had the greatest increases and decreases in predicted SDI_{MAX} relative to mixed species scenario. For example, under RCP 8.5—2080s, the average positive shift was 2.9% and 1.1% greater for the DF-Mix and HemFir data sets, respectively, under the pure basal area scenarios relative to the average basal area scenarios. Conversely, the average negative shift was −6.7% and −3.8% greater for the pure basal area scenarios relative to the average basal area scenarios for the DF-Mix and HemFir data sets, respectively.

Moving toward mixed species management could allow for greater resilience to a changing climate. Under projected future conditions, mixed stands may be able to carry a greater density longer into the rotation before the impact of density-dependent mortality. Puettmann (2011) describes this as the "insurance hypothesis" (attributed to Yachi & Loreau, 1999) under which a diversity of species and vegetation conditions may buffer the impact of a changing climate. A more diverse forest allows for complementary facilitation, where the presence of one species increases the availability of a limiting resource, and resource portioning, with more efficient sharing of limited resources between different species (Pothier, 2019).

Projected future climate scenarios fall into extramural conditions across all scenarios. Utilizing any statistical model to extrapolate or predict outside the range of the input data is not appropriate. Nonetheless, general interpretations of the overall direction and magnitude of these shifts should be considered to understand what impact future climate may have on stand carrying capacity. The impact of environmental conditions is reflected in the underlying physiographical processes of these forest communities. While it is understood that climate influences carrying capacity (Andrews et al., 2018; Kimsey et al., 2019), general interpretations of the model projections are justified with the acknowledgment of the uncertainties involved in climate projections. In particular, the consistency of the modeled relationship between climate variables and SDI_{MAX} beyond the range of input data, as well as the unknown impact of elevated CO_2 concentrations on plant growth.

5 | CONCLUSION

Climate projections show forest communities of the Pacific Northwest may be facing a longer, warmer, droughtier growing season in the future. Snowpack to provide water in some more precipitation-limited areas will be both increasingly significant and inadequate. Spatial knowledge of where these impacts will be felt the most is important for silvicultural planning. Management approaches need to consider the impacts of these changes on the forest stand's ability to handle the increase in density-dependent competition, in particular for what may be an even more limited water supply. Planting and thinning to lower densities may provide resilience and capture the projected increases in density-related mortality. Given the amount of forests at or near maximum density limits across the United States has steadily increased over the last 20 years (Woodall & Weiskittel, 2021), density management strategies need to be considered in any current and future planning. Although many unknowns remain, for example, the impact of global change on disease and insect patterns (Bentz et al., 2010) or wildfire behavior (Loehman et al., 2020), density management guidelines need to consider the influence a changing environment will have on density-driven interactions among forest communities. These results present forest managers and policy-makers with the ability to make location-specific interpretations of the magnitude and variability of potential shifts in forest stand carrying capacity.

19397445, 2023, 4, Downloaded from https://onlinelibrary.wiley.com/doi/10.1111/nrm.12381, Wiley Online Library on [29/11/2023]. See the Terms and Conditions (https://onlinelibrary.wiley.com/terms-and-conditions) on Wiley Online Library for rules of use; OA articles are governed by the applicable Creative Commons License

AUTHOR CONTRIBUTIONS

Ryan R. Heiderman: Methodology; formal analysis; validation; visualization; writing— original draft. Mark J. Kimsey: Conceptualization; funding acquisition; project administration.

ACKNOWLEDGMENTS

Data for this research was provided through a collaborative network of regional forest management cooperative members from the Intermountain Forestry Cooperative (IFC) at the University of Idaho and the Center for Intensive Planted-forest Silviculture (CIPS) at Oregon State University. We gratefully acknowledge Robyn Darbyshire and the Region 6 United States Forest Service for providing support and funding for this project. We also wish to thank the United States Forest Service FIA program for providing unfuzzed data.

DATA AVAILABILITY STATEMENT

Research data are not shared.

ORCID

Ryan R. Heiderman http://orcid.org/0009-0001-1273-5018
Mark J. Kimsey http://orcid.org/0000-0002-0358-2750

REFERENCES

Aguirre, A., del Río, M., & Condés, S. (2018). Intra- and inter-specific variation of the maximum size-density relationship along an aridity gradient in Iberian pinewoods. Forest Ecology and Management, 411, 90–100. https://doi.org/10.1016/j.foreco.2018.01.017

Andrews, C., Weiskittel, A., D'Amato, A. W., & Simons-legaard, E. (2018). Variation in the maximum stand density index and its linkage to climate in mixed species forests of the North American Acadian Region. Forest Ecology and Management, 417, 90–102. https://doi.org/10.1016/j.foreco.2018.02.038

Bentz, B. J., Régnière, J., Fettig, C. J., Hansen, E. M., Hayes, J. L., Hicke, J. A., Kelsey, R. G., Negrón, J. F., & Seybold, S. J. (2010). Climate change and bark beetles of the Western United States and Canada: Direct and indirect effects. BioScience, 60(8), 602–613. https://doi.org/10.1525/bio.2010.60.8.6

Brunet-Navarro, P., Sterck, F. J., Vayreda, J., Martinez-Vilalta, J., & Mohren, G. M. J. (2016). Self-thinning in four pine species: An evaluation of potential climate impacts. Annals of Forest Science, 73, 1025–1034. https://doi.org/10.1007/s13595-016-0585-y

Chmura, D. J., Anderson, P. D., Howe, G. T., Harrington, C. A., Halofsky, J. E., Peterson, D. L., Shaw, D. C., & Brad St.Clair, J. (2011). Forest responses to climate change in the northwestern United States: Ecophysiological foundations for adaptive management. Forest Ecology and Management, 261, 1121–1142. https://doi.org/10.1016/j.foreco.2010.12.040

Deng, J. M., Wang, G. X., Morris, E. C., Wei, X. P., Li, D. X., Chen, B. M., Zhao, C. M., Liu, J., & Wang, Y. (2006). Plant mass–density relationship along a moisture gradient in north-west China. Journal of Ecology, 94, 953–958. https://doi.org/10.1111/j.1365-2745.2006.01141.x

Dolanc, C. R., Thorne, J. H., & Safford, H. D. (2013). Widespread shifts in the demographic structure of subalpine forests in the Sierra Nevada, California, 1934 to 2007. Global Ecology and Biogeography, 22, 264–276. https://doi.org/10.1111/j.1466-8238.2011.00748.x

Elith, J., Leathwick, J. R., & Hastie, T. (2008). A working guide to boosted regression trees. Journal of Animal Ecology, 77, 802–813. https://doi.org/10.1111/j.1365.2656.2008.01390.x

Fernandes, T. J. G, Campo, A. D. D, Herrera, R, Molina, A. J. (2016). Simultaneous assessment, through sap flow and stable isotopes, of water use efficiency (WUE) in thinned pines shows improvement in growth, treeclimate

19397445, 2023, 4, Downloaded from https://onlinelibrary.wiley.com/doi/10.1111/nrm.12381, Wiley Online Library on [29/11/2023]. See the Terms and Conditions (https://onlinelibrary.wiley.com/terms-and-conditions) on Wiley Online Library for rules of use; OA articles are governed by the applicable Creative Commons License

sensitivity and WUE, but not in WUEi. Forest Ecology and Management, 361, 298–308. https://doi.org/10.1016/j.foreco.2015.11.029

Franklin, J., & Waring, R. (1980). Distinctive features of the Northwestern coniferous forest: Development, structure, and function. In W. H. Richard (Ed.), Ecosystem analysis: Proceedings of the 40th annual biological colloquim (pp. 59–86). Oregon State University Press, Corvallis, OR.

Friedman, J. H. (2001). Greedy function approximation: A gradient boosting machine. The Annals of Statistics, 29(5), 1189–1232. https://doi.org/10.1214/aos/1013203451

Geraci, M. (2014). Linear quantile mixed models: The 'lqmm' package for Laplace quantile regression. Journal of Statistical Software, 57(3), 1–29. https://doi.org/10.18637/jss.v057.i13

Gleason, K. E., Bradford, J. B., D'amato, A. W., Fraver, S., Palik, B. J., & Battaglia, M. A. (2021). Forest density intensifies the importance of snowpack to growth in water-limited pine forests. Ecological Applications: A Publication of the Ecological Society of America, 31(1), 02211. https://doi.org/10.1002/eap.2211

Greenwell, B., Boehmke, B., & Cunningham, J., & GBM Developers. (2020). gbm: Generalized boosted regression models. R package version 2.1.8. https://CRAN.R-project.org/package=gbm

Harpold, A. A. (2016). Diverging sensitivity of soil water stress to changing snowmelt timing in the Western U.S. Advances in Water Resources, 92, 116–129. https://doi.org/10,1016/j.advwatres.2016.03.017

Hastie, T., Tibshirani, R., & Friedman, R. (2008). The elements of statistical learning: Data mining, inference, and prediction (2nd ed.). Springer.

Hijmans, R. (2020). 'raster': Geographic data analysis and modeling. R package version, 3 (pp. 3–13). https://CRAN.R-project.org/package=raster

IPCC. (2013). Climate change 2013: The physical science basis. In T. F. Stocker, D. Qin, G.-K. Plattner, M. Tignor, S. K. Allen, J. Boschung, A. Nauels, Y. Xia, V. Bex, & P. M. Midgley (Eds.), Contribution of working group I to the fifth assessment report of the intergovernmental panel on climate change (1535pp.). Cambridge University Press. https://doi.org/10.1017/CBO9781107415324

Iverson, L. R., Prasad, A. M., Matthews, S. N., & Peters, M. (2008). Estimating potential habitat for 134 eastern US tree species under six climate scenarios. Forest Ecology and Management, 254, 390–406. https://doi.org/10.1016/j.foreco.2007.07.023

Kimsey, M. J., Shaw, T. M., & Coleman, M. D. (2019). Site sensitive maximum stand density index models for mixed conifer stands across the Inland Northwest, USA. Forest Ecology and Management, 433, 396–404. https://doi.org/10.1016/j.foreco.2018.11.013

Klos, P. Z., Link, T. E., & Abatzoglou, J. T. (2014). Extent of the rain–snow transition zone in the western U.S. under historic and projected climate: Climatic rain–snow transition zone. Geophysical Research Letters, 41, 4560–4568. https://doi.org/10.1002/2014GL060500

Kuhn, M. (2020). caret: Classification and Regression Training. R package version 6.0-86. https://CRAN.R-project.org/package=caret

Loehman, R. A., Keane, R. E., & Holsinger, L. M. (2020). Simulation modeling of complex climate, wildfire, and vegetation dynamics to address wicked problems in land management. Frontiers in Forests and Global Change, 3, 1–13. https://doi.org/10.3389/ffgc.2020.00003

Millar, C. I., Stephenson, N. L., & Stephens, S. L. (2007). Climate change and forests of the future: Managing in the face of uncertainty. Ecological Applications, 17(8), 2145–2151. https://doi.org/10.1890/06-1715.1

Parmesan, C. (2006). Ecological and evolutionary responses to recent climate change. Annual Review of Ecology, Evolution, and Systematics, 37, 637–669. https://doi.org/10.1146/annurev.ecolsys.37.091305.110100

Pothier, D. (2019). Analysing the growth dynamics of mixed stands composed of balsam fir and broadleaved species of various shade tolerances. Forest Ecology and Management, 444, 21–29. https://doi.org/10.1016/j.foreco.2019.04.035

19397445, 2023, 4, Downloaded from https://onlinelibrary.wiley.com/doi/10.1111/nrm.12381, Wiley Online Library on [29/11/2023]. See the Terms and Conditions (https://onlinelibrary.wiley.com/terms-and-conditions) on Wiley Online Library for rules of use; OA articles are governed by the applicable Creative Commons License

Pretzsch, H., & Biber, P. (2016). Tree species mixing can increase maximum stand density. Canadian Journal of Forest Research, 46(10), 1179–1193. https://doi.org/10.1139/cjfr-2015-0413

Puettmann, K. (2011). Silvicultural challenges and options in the context of global change: "Simple" fixes and opportunities for new management approaches. Journal of Forestry, 109(6), 321–331. https://doi.org/10.1093/jof/109.6.321

R Core Team. (2020). R: A language and environment for statistical computing. R Foundation for Statistical Computing. https://www.R-project.com

Rehfeldt, G. E., Crookston, N. L., Warwell, M. V., & Evans, J. S. (2006). Empirical analyses of plant–climate relationships for the western United States. International Journal of Plant Sciences, 167(6), 1123–1150. https://doi.org/10.1086/507711

Reineke, L. (1933). Perfecting a stand-density index for even-aged forests. Journal of Agricultural Research, 46(7), 627–638.

Roise, J., & Betters, D. (1981). An aspect transformation with regard to elevation for site productivity models. Forest Science, 27(3), 483–486. https://doi.org/10.1093/forestscience/27.3.483

Salas-Eljatib, C., & Weiskittel, A. R. (2018). Evaluation of modeling strategies for assessing self-thinning behavior and carrying capacity. Ecology and Evolution, 8, 10768–10779. https://doi.org/10.1002/ece3.4525

van Vuuren, D. P., Edmonds, J., Kainuma, M., Riahi, K., Thomson, A., Hibbard, K., Hurtt, G. C., Kram, T., Krey, V., Lamarque, J. F., Masui, T., Meinshausen, M., Nakicenovic, N., Smith, S. J., & Rose, S. K. (2011). The representative concentration pathways: An overview. Climatic Change, 109, 5–31. https://doi.org/10.1007/s10584-011-0148-z

Wang, T., Hamann, A., Spittlehouse, D., & Carroll, C. (2016). Locally downscaled and spatially customizable climate data for historical and future periods for North America. PLoS One, 11(6), 1–17. https://doi.org/10.1371/journal.pone.0156720

Waring, R. H., & Franklin, J. F. (1979). Evergreen coniferous forests of the Pacific Northwest. Science, 204, 1380–1386. https://doi.org/10.1126/science.204.4400.1380

Way, D. A., & Oren, R. (2010). Differential responses to changes in growth temperature between trees from different functional groups and biomes: A review and synthesis of data. Tree Physiology, 30, 669–688. https://doi.org/10/1093/treephys/tpq015

Woodall, C. W., & Weiskittel, A. R. (2021). Relative density of United States forests has shifted to higher levels over last two decades with important implications for future dynamics. Scientific Reports, 11, 18848. https://doi.org/10.1038/s41598-021-98244-w

Yachi, S., & Loreau, M. (1999). Biodiversity and ecosystem productivity in a fluctuating environment: The insurance hypothesis. Proceedings of the National Academy of Sciences of the United States of America, 96(4), 1463–1468. https://doi.org/10.1073/pnas.96.4.1463

Yue, C., Kahle, H. P., von Wilpert, K., & Kohnle, U. (2016). A dynamic environment-sensitive site index model for the prediction of site productivity potential under climate change. Ecological Modelling, 337, 48–62. https://doi.org/10.1016/j.ecolmodel.2016.06.005

How to cite this article: Heiderman, R. R., & Kimsey, Jr. M. J. (2023). Pacific Northwest conifer forest stand carrying capacity under future climate scenarios. Natural Resource Modeling, 36, e12381. https://doi.org/10.1111/nrm.12381

APPENDIX A

(see Tables A1 and A2)

19397445, 2023, 4, Downloaded from https://onlinelibrary.wiley.com/doi/10.1111/nrm.12381, Wiley Online Library on [29/11/2023]. See the Terms and Conditions (https://onlinelibrary.wiley.com/terms-and-conditions) on Wiley Online Library for rules of use; OA articles are governed by the applicable Creative Commons License

TABLE A1 Absolute change in temperature (°C) under future climate scenarios relative to historical for the current range of DF-Mix and HemFir.

		DF-Mix					HemFir						
Scenario	Variable	Min	1%	Med	Mean	99%	Max	Min	1%	Med	Mean	99%	Max
RCP 4.5—2050s	MCMT	1.6	1.7	2.0	2.0	2.5	2.6	1.6	1.8	2.1	2.1	2.5	2.6
	MWMT	2.2	2.3	2.7	2.7	3.1	3.2	2.2	2.3	2.9	2.8	3.1	3.2
RCP 4.5—2080s	MCMT	2.0	2.1	2.5	2.5	3.0	3.2	2.0	2.1	2.5	2.6	3.0	3.1
	MWMT	2.8	2.9	3.4	3.4	4.0	4.1	2.8	2.9	3.6	3.5	4.0	4.1
RCP 8.5—2050s	MCMT	2.0	2.1	2.4	2.5	3.1	3.2	2.0	2.1	2.5	2.6	3.1	3.2
	MWMT	2.9	3.0	3.6	3.6	4.2	4.3	2.9	3.0	3.8	3.7	4.2	4.3
RCP 8.5—2080s	MCMT	3.4	3.5	4.0	4.0	4.9	5.1	3.4	3.6	4.1	4.2	4.9	5.1
	MWMT	4.6	4.9	5.8	5.8	6.8	6.9	4.7	4.9	6.2	6.0	6.8	6.9

Abbreviations: Max, maximum; MCMT, mean coldest month temperature; Med, medium; Min, minimum; MWMT, mean warmest month temperature.

19397445, 2023, 4, Downloaded from https://onlinelibrary.wiley.com/doi/10.1111/nrm.12381, Wiley Online Library on [29/11/2023]. See the Terms and Conditions (https://onlinelibrary.wiley.com/terms-and-conditions) on Wiley Online Library for rules of use; OA articles are governed by the applicable Creative Commons License

TABLEA2 Percentchangeinimportantclimatevariablesunderfutureclimatescenariosforthecurrentrangesof DF ¯MixandHemFirrelativetohistoricalclimate conditions.

RCP 4.5—2050s	MAP	−2%	−1%	1%	1%	4%	4%	−2%	−1%	1%	1%	4%	4%
	PRATIO	−14%	−12%	−10%	−10%	−8%	−7%	−13%	−11%	−9%	−9%	−8%	−7%
	PAS	−64%	−61%	−54%	−54%	−36%	−15%	−63%	−61%	−55%	−55%	−41%	−26%
	DD5	20%	23%	30%	33%	57%	96%	23%	27%	34%	36%	53%	69%
	FFP	17%	21%	26%	27%	42%	86%	18%	22%	27%	27%	37%	49%
RCP 4.5 - 2080s	MAP	−1%	0%	2%	3%	6%	7%	−1%	0%	3%	3%	6%	7%
	PRATIO	−15%	−13%	−11%	−11%	−9%	−8%	−15%	−13%	−11%	−11%	−9%	−8%
	PAS	−70%	−68%	−61%	−61%	−43%	−18%	−69%	−67%	−62%	−62%	−49%	−31%
	DD5	26%	29%	39%	42%	74%	129%	29%	34%	43%	45%	68%	86%
	FFP	21%	26%	33%	34%	53%	117%	22%	28%	34%	35%	46%	63%
RCP 8.5—2050s	MAP	−2%	−1%	2%	2%	5%	6%	−2%	−1%	3%	2%	5%	6%
	PRATIO	−16%	−14%	−12%	−12%	−10%	−9%	−15%	−14%	−12%	−12%	−10%	−9%
	PAS	−71%	−70%	−63%	−63%	−45%	−20%	−71%	−69%	−64%	−64%	−51%	−34%
	DD5	27%	31%	40%	44%	79%	139%	30%	36%	45%	48%	72%	92%
	FFP	21%	26%	35%	35%	55%	124%	23%	30%	35%	36%	48%	65%

DF_MixHemFir

ScenarioVariableMin1%MedMean99%MaxMin1%MedMean99%Max

19397445, 2023, 4, Downloaded from https://onlinelibrary.wiley.com/doi/10.1111/nrm.12381, Wiley Online Library on [29/11/2023]. See the Terms and Conditions (https://onlinelibrary.wiley.com/terms-and-conditions) on Wiley Online Library for rules of use; OA articles are governed by the applicable Creative Commons License

)

TABLEA2 Continued

(		DF¯MixHemFir											
Scenario	Variable	Min	1%	Med	Mean	99%	Max	Min	1%	Med	Mean	99%	Max
sMAP		0%	1%	4%	4%	8%	10%	0%	1%	5%	5%	8%	10%
RCP8.5 ¯													
	PRATIO	¯19%	¯18%	¯15%	¯15%	¯13%	¯12%	¯19%	¯17%	¯15%	¯15%	¯13%	¯12%
	PAS	¯87%	¯85%	¯80%	¯80%	¯67%	¯38%	¯87%	¯84%	¯80%	¯80%	¯71%	¯56%
	DD5	44%	50%	67%	73%	136%	244%	49%	58%	74%	79%	124%	160%
	FFP	27%	39%	57%	57%	87%	210%	32%	46%	59%	59%	77%	103%

Abbreviations:DD5,degreedaysabove5°C;FFP,frost ¯freeperiod;MAP,meanannualprecipitation;Max,maximum;Med,median;Min,minimum;PAS,precipitationassnow; PRATIO,proportionofprecipitationfallingduringthegrowingseason.